

Supporting Information for

Heteroepitaxial Growth and Interface Band Alignment in Large-Mismatch CsPbI₃/GaN Heterojunction

Xueyin Liu^a, Dan Cao^{a,*}, Yizhou Yao^a, Pengtao Tang^b, Mingsong Zhang^b, Xiaoshuang
Chen^c, and Haibo Shu^{b,*}

^aCollege of Science and ^bCollege of Optical and Electronic Technology, China Jiliang
University, 310018 Hangzhou, China.

^cNational Laboratory for Infrared Physics, Shanghai Institute of Technical Physics,
Chinese Academy of Science, 200083 Shanghai, China

*Corresponding authors (Dan Cao, email : caodan@cjlu.edu.cn; Haibo Shu, email :
shuhaibo@cjlu.edu.cn)

S1. The influence of growth parameters on the growth of CsPbI₃ on GaN

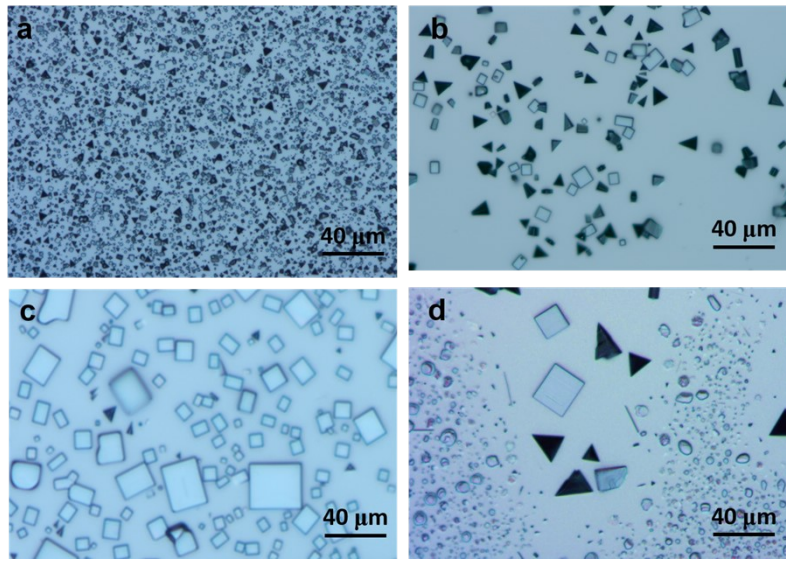


Fig. S1 OM images of CsPbI₃ grown on GaN substrate with the growth temperature of (a) 660 °C, (b) 680 °C, (c) 700 °C, and (d) 720 °C. The scale bar is 40 μm. The gas flow is set at 80 sccm.

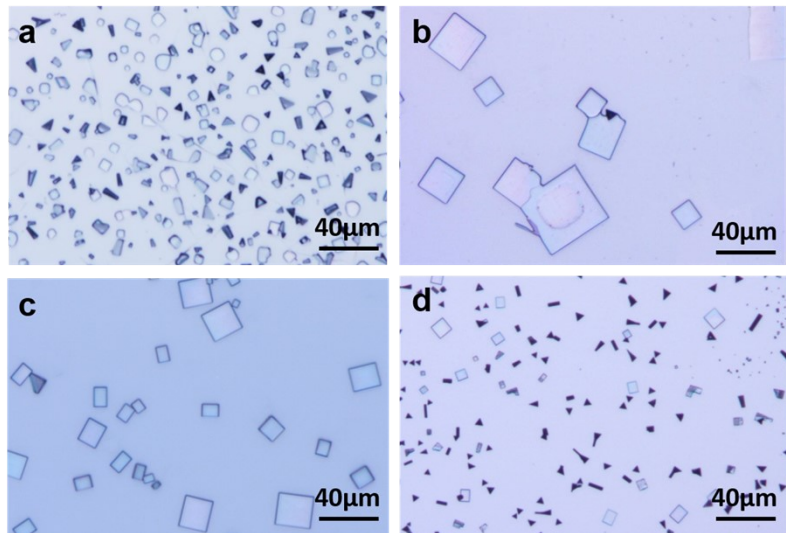


Fig. S2 OM images of CsPbI₃ grown on GaN substrate with the Ar-gas flow of (a) 40 sccm, (b) 60 sccm, (c) 80 sccm, and (d) 100 sccm. The scale bar is 40 μm. The growth temperature is set at 700 °C.

S2. Size-distribution statistics of CsPbI₃ grown on GaN

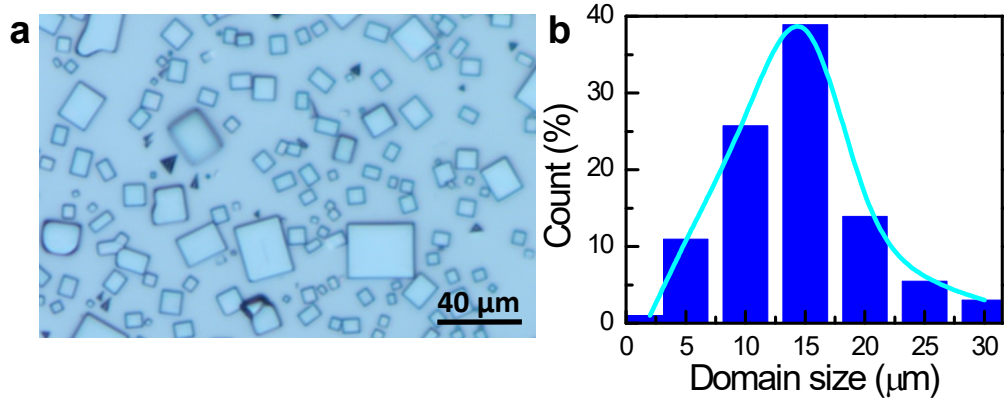


Fig. S3 (a) A large-area OM image of CsPbI₃ NPs grown on GaN substrate. (b) Statistics on the domain size of as-grown CsPbI₃ NPs on GaN in a selected area of 200×200 μm².

S3. Morphological characterizations of CsPbI₃ grown on mica substrate

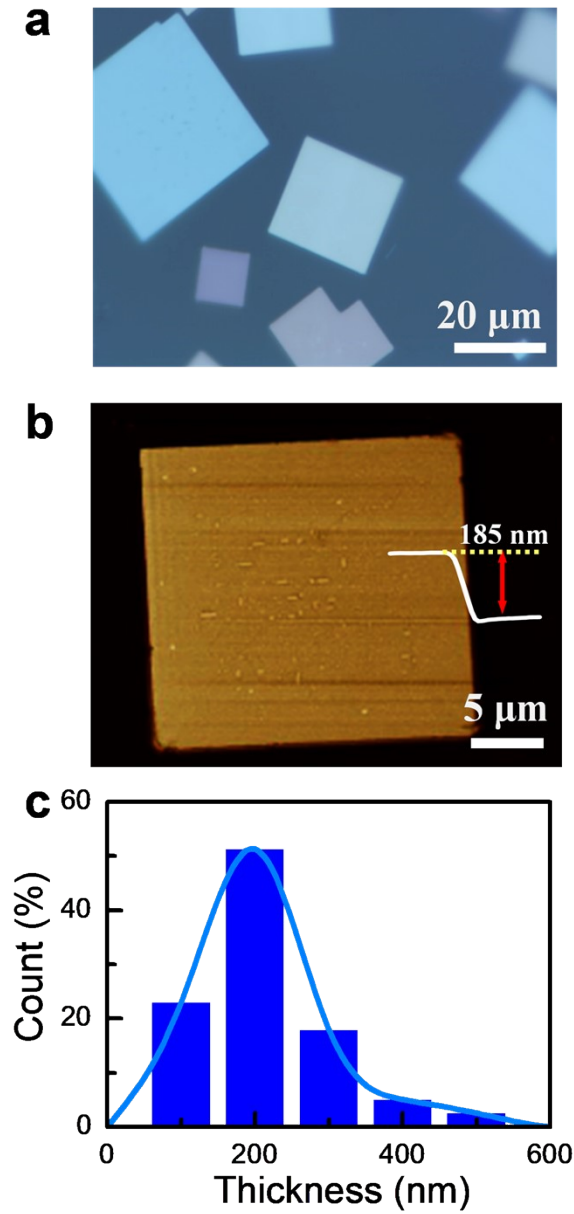


Fig. S4 (a) OM image of CsPbI₃ NPs grown on mica substrate. (b) AFM image and height profile of a CsPbI₃ NP. (c) Statistics on the thickness of as-grown CsPbI₃ NPs in a selected area of 200×200 μm² on mica substrate.

S4. EDS element analysis and SEM image of CsPbI₃ grown on GaN

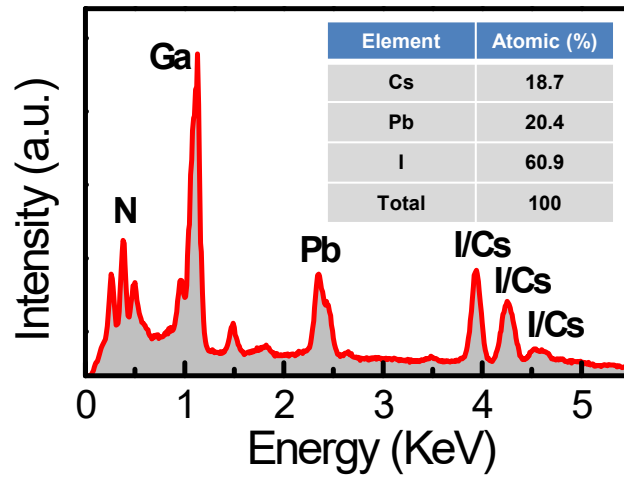


Fig. S5 Element analysis of CsPbI₃ NPs grown on GaN substrate from EDS measurement result. Inset: the atomic ratio of CsPbI₃.

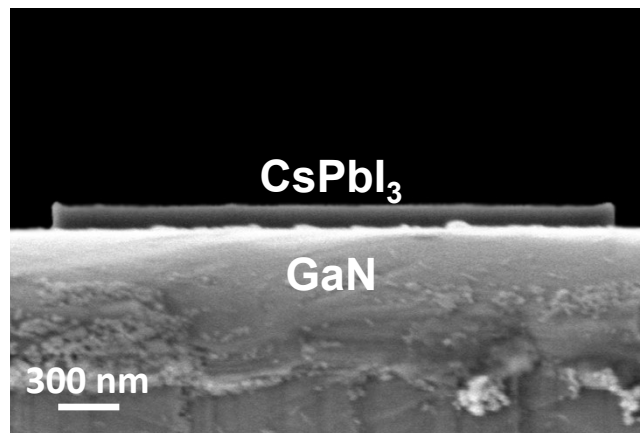


Fig. S6 The SEM image of the cross-section of CsPbI₃/GaN heterojunction. The scale bar is 300 nm.

S5. XRD pattern of GaN/sapphire substrate

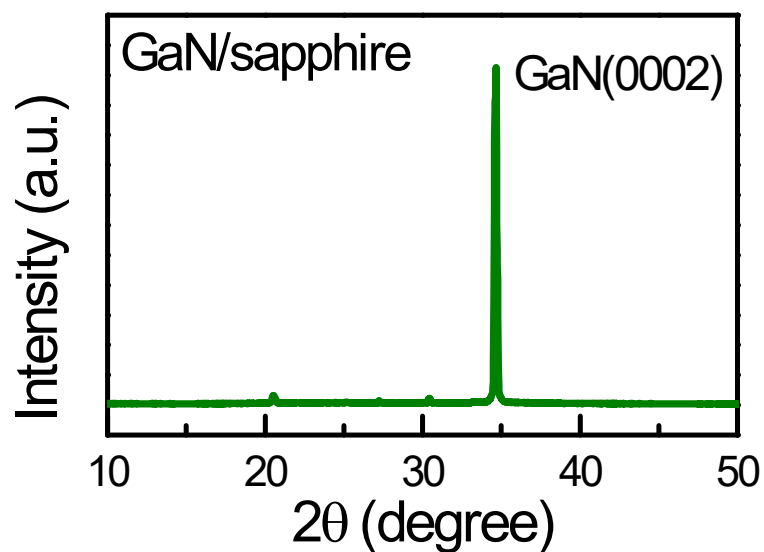


Fig. S7 XRD pattern of GaN/sapphire substrate. The sharp diffraction peaks assigned at 34.5° is well-indexed to the (0002) plane of GaN.

S6. Atomic structure of GaN(0001) surface

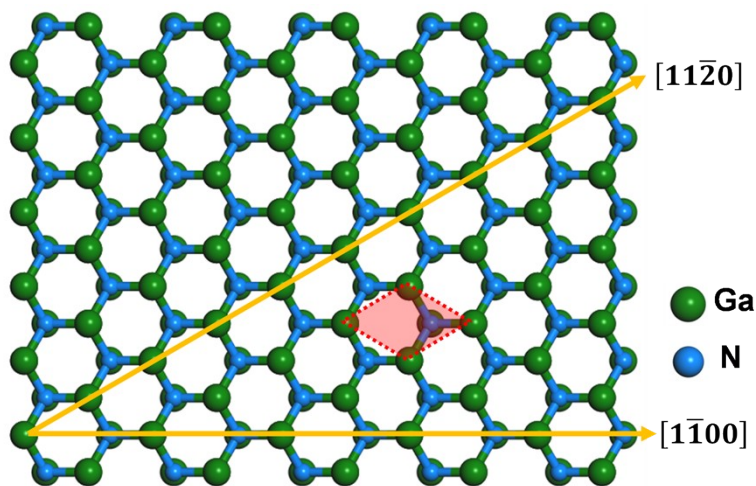


Fig. S8 Top view of atomic structure of GaN(0001) surface. The red region indicates the range of a GaN unit cell. The direction of arrows shows two important surface orientations: [1-100] and [11-20]. The green and blue balls denote Ga and N atoms, respectively.

S7. XRD and Raman spectra of CsPbI₃ grown on mica

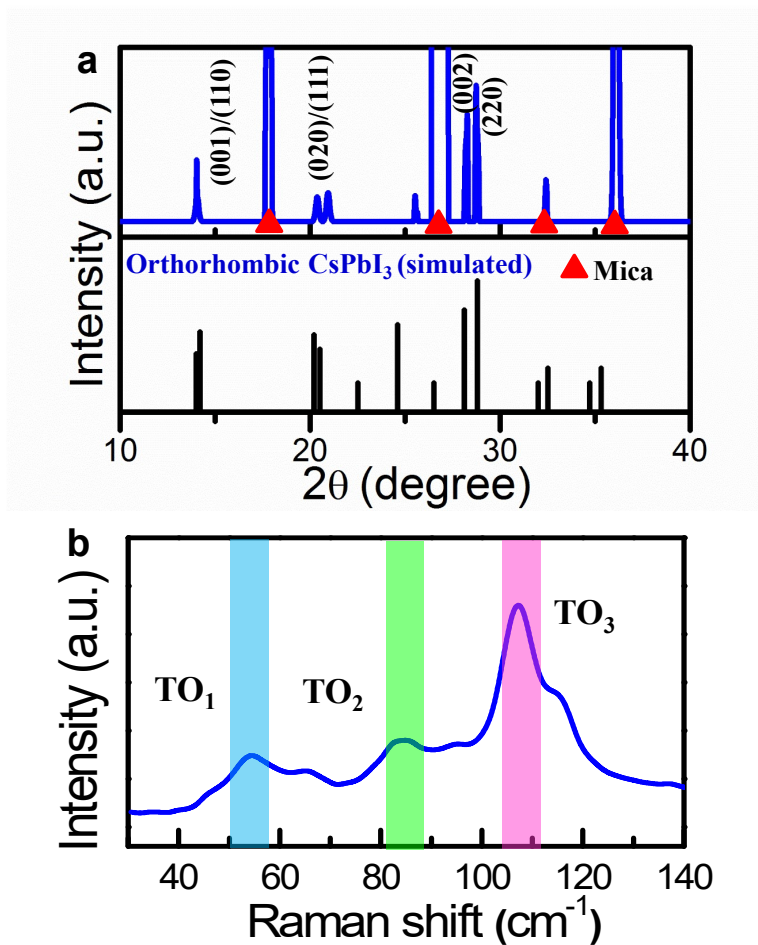


Fig. S9 (a) XRD pattern of the as-grown CsPbI₃ NPs on mica substrate. The XRD pattern of standard orthorhombic-phase CsPbI₃ from the simulation [26] is used as a reference. The diffraction peaks of mica substrate are labeled by red triangles. (b) Raman spectra of CsPbI₃ NPs grown on mica substrate. The main Raman peaks (i.e., TO₁, TO₂, and TO₃ modes) have been emphasized by the shadow regions.

S8. XPS and absorbance spectra of CsPbI₃ grown on GaN and mica substrates

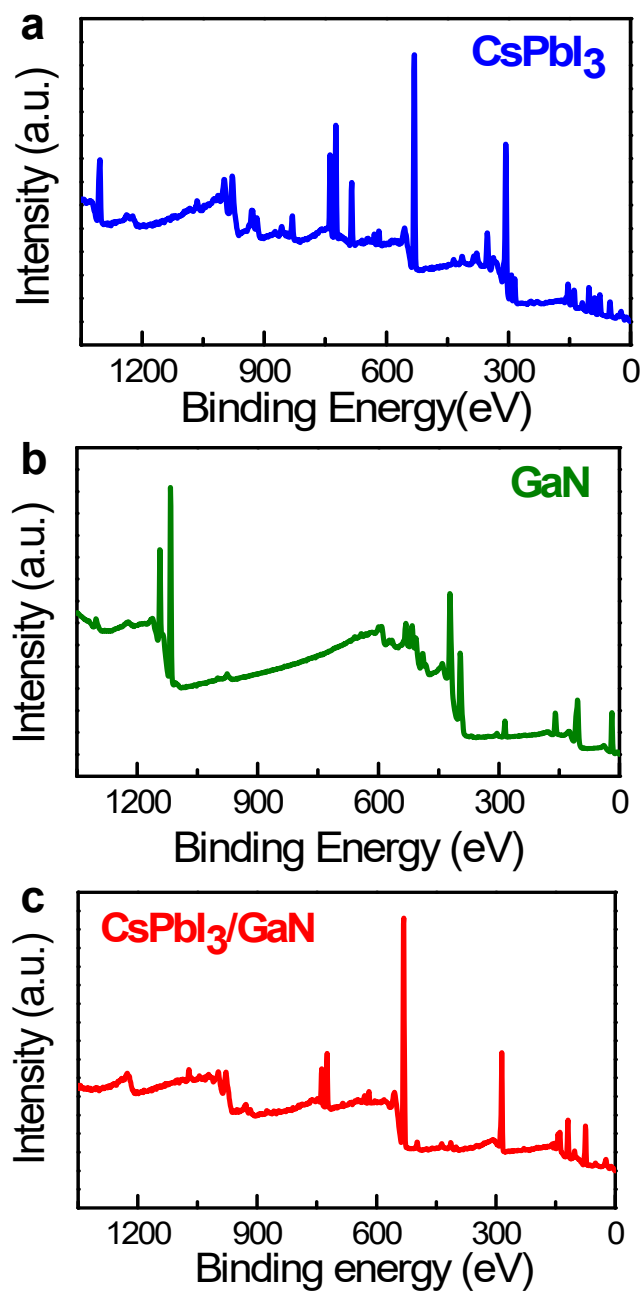


Fig. S10 XPS spectra of (a) CsPbI₃ NPs, (b) GaN substrate, and (c) CsPbI₃/GaN heterojunction

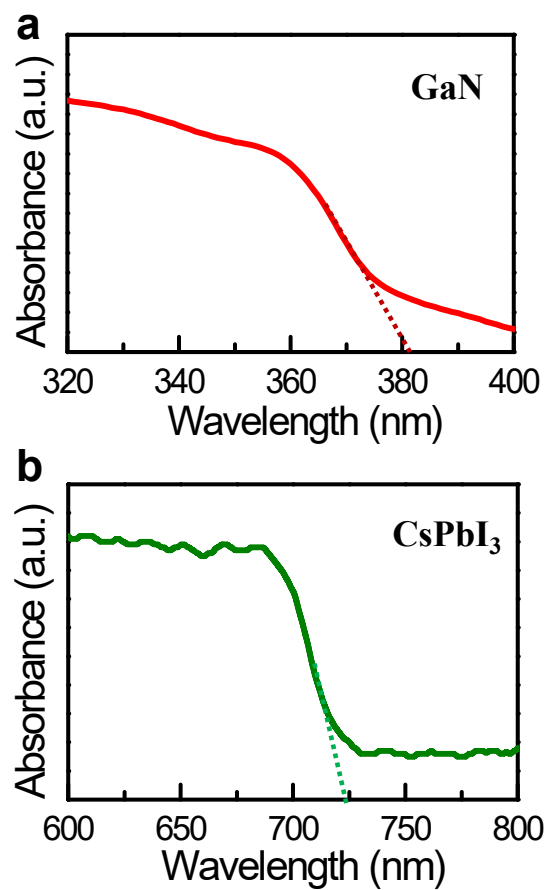


Fig. S11 Absorbance spectra of (a) GaN substrate and (b) CsPbI₃ NPs. The absorption edge of GaN and CsPbI₃ is 382 nm and 725 nm, respectively.

S9. DFT calculations of Band structure and carrier mobility

Computational methods: All DFT calculations were performed using the projector augmented wave (PAW) method¹ as implemented in the Vienna *ab initio* Simulation Package (VASP)^{2,3}. The electronic exchange and correlation were described by the generalized-gradient approximation (GGA) with the Perdew-Burke-Ernzerh (PBE) version⁴. The cutoff energy of the plane wave basis was set to 500 eV. Since the GGA-PBE functional underestimates the band gaps of semiconductor materials, the hybrid Heyd-Scuseria-Ernzerhof (HSE06) functional⁵ was used to obtain electronic structures of CsPbI₃ and GaN. Moreover, the spin-orbit coupling (SOC) was also considered in the calculations of CsPbI₃. The k -point sampling in the Brillouin zone was implemented by the Monkhorst-Pack scheme with the grid of $12 \times 12 \times 8$ for the orthorhombic CsPbI₃ and $16 \times 16 \times 10$ for the wurtzite GaN, respectively. All geometry optimizations were performed using the conjugate-gradient method and the convergence criteria of energy and force were set to 10^{-4} eV/atom and 10^{-2} eV/Å, respectively.

The calculation of carrier mobility: The carrier mobilities of CsPbI₃ and GaN were calculated by deformation potential (DP) theory⁶. According to the DP theory, the room-temperature carrier mobility (μ) of the orthorhombic CsPbI₃ and wurtzite GaN can be estimated by using the acoustic phonon-limited approach with the following equation,

$$\mu_a = \frac{2^{3/2} \pi^{1/2} \hbar C_a}{3(k_B T)^{3/2} |m_a^*|^{3/2} |m_b^*|^{1/2} |m_c^*|^{1/2} E_{1a}^2} \quad (1)$$

$$\mu_b = \frac{2^{3/2} \pi^{1/2} \hbar C_b}{3(k_B T)^{3/2} |m_a^*|^{1/2} |m_b^*|^{3/2} |m_c^*|^{1/2} E_{1b}^2} \quad (2)$$

$$\mu_c = \frac{2^{3/2} \pi^{1/2} \hbar C_c}{3(k_B T)^{3/2} |m_a^*|^{1/2} |m_b^*|^{1/2} |m_c^*|^{3/2} E_{1c}^2} \quad (3)$$

where m_i^* ($i = a, b, c$) is the effective mass along the i -axis transport direction. E_l is the DP constant that denotes the shift of the band edges (the maximum of valence band for holes and the minimum of conduction band for electrons) induced by the strain in the range of $\pm 1\%$, C_{2D} is the elastic constant. \hbar is the reduced Planck constant, k_B is Boltzmann constant, and T is the temperature that is set to 298 K (i.e., room temperature).

Based on the equation (1)-(3), the carrier mobilities of CsPbI₃ and GaN can be obtained, as listed in Table S1.

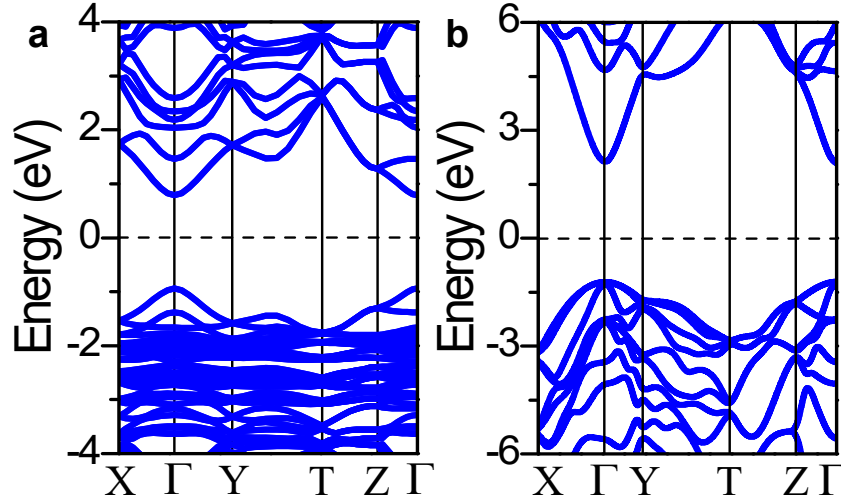


Fig. S12 Electronic band structure of (a) orthorhombic CsPbI₃ and (b) wurtzite GaN calculated by the HSE06 functional. For the calculation of orthorhombic CsPbI₃, the spin-orbital coupling effect is also included. The dash lines denote the position of Fermi level.

Table S1 Carrier effective masses (m_e^* and m_h^*) and carrier mobility (μ_e and μ_h) of orthorhombic CsPbI₃ and wurtzite GaN. Here a , b , c corresponds to three components along a -axis, b -axis, and c -axis directions, respectively.

Material	$m_e^* (m_0)$			$m_h^* (m_0)$			$\mu_e (\text{cm}^2\text{V}^{-1}\text{s}^{-1})$			$\mu_h (\text{cm}^2\text{V}^{-1}\text{s}^{-1})$		
	a	b	c	a	b	c	a	b	c	a	b	c
CsPbI ₃	0.38	0.35	0.36	0.42	0.46	0.47	1503	881	2773	576	486	661
GaN	0.22	0.20	0.19	1.85	1.62	1.91	2696	2130	2560	33	27	40

S10. PL spectra of CsPbI₃ grown on GaN before and after transferred onto SiO₂/Si

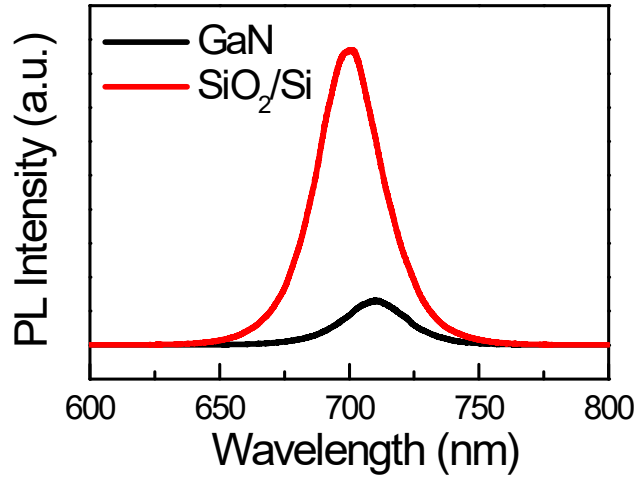


Fig. S13 PL spectra of CsPbI₃ NP grown on GaN substrate before (black) and after (red) transferred onto SiO₂/Si substrate under the same excitation condition. Here the CsPbI₃ NPs were transferred from GaN substrate to SiO₂/Si substrate by a dry-transfer technique. More specifically, the PDMS was firstly fabricated from Sylgard 184 silicone elastomer (Dow Corning Corp.) mixed with curing agent using a ratio of 10:1. The PDMS was pressed to make full contact with CsPbI₃-GaN for 30 min, and then the PDMS with CsPbI₃ crystal flakes was transferred and quickly contacted with the SiO₂/Si substrate. After pressing the surface for 10 min, the PDMS film was stripped slowly from the surface of SiO₂/Si substrate, making the CsPbI₃ NPs left on the SiO₂/Si substrate.

S11. Temperature-dependent PL spectroscopy of CsPbI₃ on mica

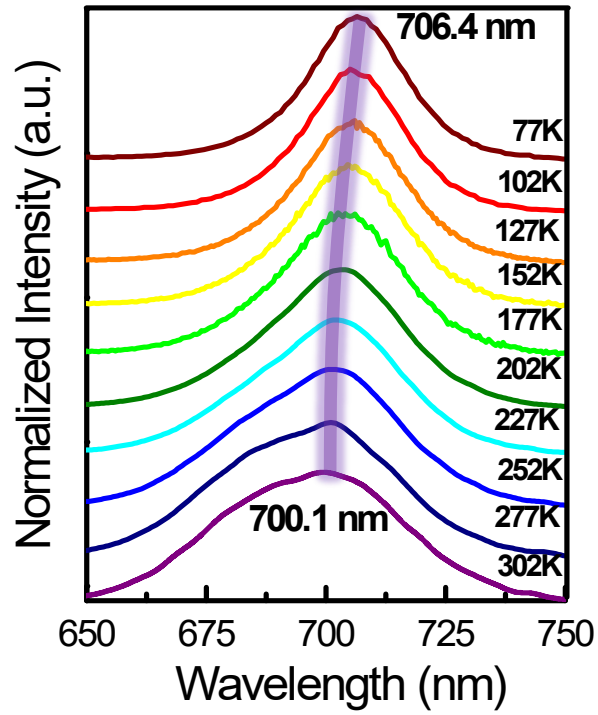


Fig. S14 Temperature-dependent PL spectroscopy of CsPbI₃ NPs grown on mica substrate with the range of measured temperature from 77 to 303 K.

S12. Fitting results of TRPL spectra

Table S2 The fitting results of TRPL spectra of CsPbI₃ NPs grown on mica and GaN substrates.

	τ_1 (ns)	τ_2 (ns)	τ_3 (ns)	A_1	ω_1 (%)	A_2	ω_2 (%)	A_3	ω_3 (%)
Mica	16.77	157.59	\	0.48	32.2	1.01	67.8	\	\
GaN	31.29	131.68	8.86	0.79	20.2	0.53	14.1	2.44	65.7

S13. The evaluation of ambient stability of CsPbI₃ grown on GaN substrate

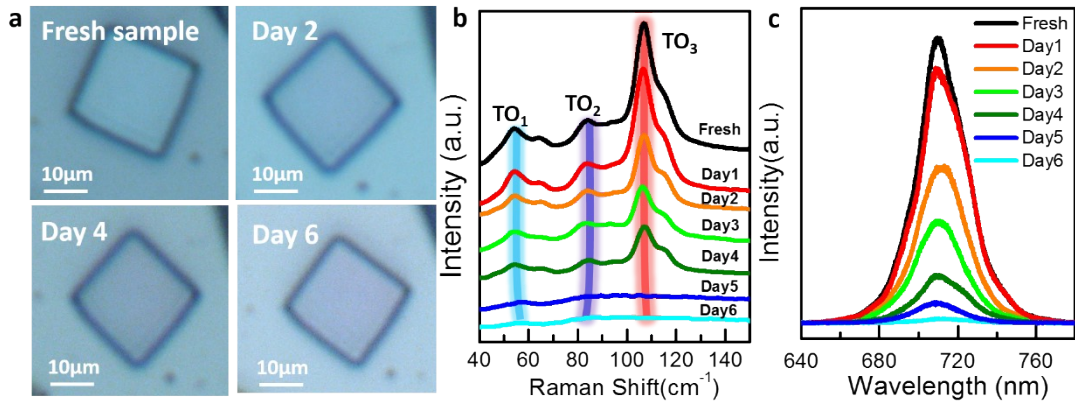


Fig. S15 The time-dependent (a) OM images, (b) Raman spectra, (c) PL spectra of CsPbI₃ grown on GaN substrate. The scale bar in OM images is 10 μm. The main Raman peaks (i.e., TO₁, TO₂, and TO₃ modes) have been emphasized by the shadow regions.

References

- [1] G. Kresse and D. Joubert, *Phys. Rev. B*, **1999**, 59, 1758-1775.
- [2] P. E. Blöchl, *Phys. Rev. B*, **1994**, 50, 17953-17979.
- [3] G. Kresse and J. Furthmüller, *Phys. Rev. B*, **1996**, 54, 11169-11185.
- [4] M.C. Payne, M.P. Teter, D.C. Allan, T.A. Arias and J. D. Joannopoulos, *Rev. Mod. Phys.*, **1992**, 64, 1045-1097.
- [5] J. Paier, M. Marsman, K. Hummer, G. Kresse, I.C. Gerber and J.G. Ángyán, *J. Chem. Phys.*, **2006**, 124, 154709.
- [6] J. Bardeen and W. Shockley, *Phys. Rev. B*, **1950**, 80, 72-80.